Harmonic generations in an optical Fibonacci superlattice

Jing Feng and Yong-yuan Zhu
Laboratory of Solid State Microstructures, Nanjing University, Nanjing 210 008, Jiangsu, People's Republic of China

Nai-ben Ming*
Laboratory of Solid State Microstructures, Nanjing University, Nanjing 210 008, Jiangsu, People's Republic of China and Center of Condensed Matter Physics and Radiation Physics, China Center of Advanced Science and Technology (World Laboratory), P.O. Box 8730, Beijing 100 080, People's Republic of China

(Received 5 April 1989; revised manuscript received 28 November 1989)

An optical Fibonacci superlattice has been proposed to produce the second-harmonic generation and the third-harmonic generation, which is the sum frequency of the second-harmonic and the fundamental frequency in the same material. Because of the quasiperiodicity of the optical Fibonacci superlattice, the phase mismatches of the optical parametric processes caused by the frequency dispersion of the refractive index can be compensated with the reciprocal vectors which the optical Fibonacci superlattice provides. A theory which analyzes the second-harmonic generation and the third-harmonic generation processes in the material and the calculations applied to the optical Fibonacci superlattice made from a single $LiNbO_3$ crystal is presented in detail. The calculations show that the efficiencies of the second-harmonic generation and the third-harmonic generation are comparable to, or even larger than, those obtained with commonly used phase-matching methods.

I. INTRODUCTION

In conventional methods, only when the phase-matching condition is satisfied does an optical parametric interaction proceed efficiently. Normally, phase matching may be realized in nonlinear optical crystals with birefringence. This method can only be applied to some of the nonlinear processes in uniaxial or biaxial crystals. Another method, quasi-phase-matching,[1,2] can be applied to both the nonbirefringent crystals and some birefringent crystals with optical coefficients that are phase unmatchable.[3-7] The key to quasi-phase-matching is to construct a one-dimensional periodic structure with the phase sign of the nonlinear polarization shifted from one plate to the consecutive plate by π radians. This one-dimensional periodic structure can provide a series of reciprocal vectors, each of which is an integer times a primitive vector. It is the reciprocal vectors which make the optical parametric processes in the material phase matched.

Compared with the periodic structure, a one-dimensional quasiperiodic structure has a low space-group symmetry. But its symmetry is higher than that of an aperiodic structure.[8-10] Its reciprocal vectors are governed by two integers rather than by one integer as in the case of the periodic one. By using this kind of material, some coupled optical parametric processes may be realized with efficient conversion.

Applying our theory to , as an example, a single $LiNbO_3$ crystal with quasiperiodic laminar ferroelectric-domain structures or simply termed an optical Fibonacci superlattice (OFS), where the nonlinear coefficient d_{33} is to be used, we find the enhancement of the second-harmonic generation (SHG) in the OFS is larger than that of an aperiodic structure, but less than that of the periodic one. We also find that the third-harmonic generation (THG), which is coupled with the SHG, can be obtained because the reciprocal vectors of such a material have more chosen values than those of the periodic one and its intensity will be large enough to be used practically and efficiently if the parameters of the building blocks are properly designed.

II. THEORETICAL ANALYSIS

Hereafter we shall take $LiNbO_3$ crystals with laminar ferroelectric-domain structures as an example. In such a material, the directions of polarization vectors in successive domains are opposite, as are the signs of nonlinear optical coefficients. This structure forms a one-dimensional superlattice for the nonlinear optical effect. On this basis, an optical Fibonacci superlattice can be constructed. It consists of two fundamental blocks of A and B arranged according to the production rule $S_j=S_{j-1}|S_{j-2}$, for $j\geq 3$ with $S_1=A$ and $S_2=AB$, where $|$ stands for concatenation. Both blocks are composed of one positive and one negative ferroelectric domain as shown in Fig. 1(a), where l_A^+ and l_B^+ represent the thicknesses of the positive domains in blocks A and B, and l_A^- and l_B^- represent the thicknesses of the negative ones. Let

$$\begin{aligned} l_A^+ &= l_B^+ = l \ , \\ l_A^- &= l(1+\delta) \ , \\ l_B^- &= l(1-t\delta) \ , \end{aligned} \tag{1}$$

l, δ, and t, are adjustable structure parameters. The sequence of the blocks, $ABAABABA\cdots$, produces an OFS, see Fig. 1(b).

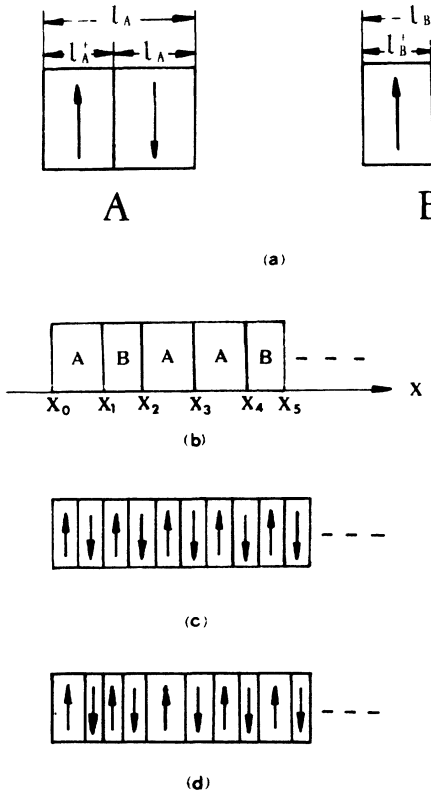

FIG. 1. Optical superlattice of $LiNbO_3$ crystals (the arrows indicate the directions of the spontaneous polarization). (a) The two blocks of an OFS, each composed of one positive and one negative ferroelectric domain. (b) Schematic diagram of an OFS. (c) Schematic diagram of a POS. (d) Schematic diagram of an APOS.

With the OFS, a series of reciprocal vectors can be provided to compensate the phase mismatches of the optical parametric processes in the material. Unlike the periodic optical superlattice (POS) [Fig. 1 (c)] which has reciprocal vectors derived from an integer times a primitive vector, an OFS with an infinite number of blocks provides reciprocal vectors governed by two integers, which has the form

$$k_{m,n}=2\pi(m+n\tau)/D \ , \tag{2}$$

where $D=\tau l_A+l_B$, with the golden ratio $\tau\equiv(1+\sqrt{5})/2$; l_A, l_B are block thicknesses as shown in Fig. 1(a). The reciprocal vectors of the OFS can be adjusted by l, δ, and t. Because of this property, some coupled optical parametric processes will be likely to occur in the OFS with efficient conversion.

Consider a case in which a single laser beam with $\omega_1=\omega$ is incident from the left onto the surface of an OFS and, through the nonlinear optical effect, the SHG and the THG exist simultaneously in the OFS. In order to make use of the largest nonlinear coefficient d_{33}, which cannot be used in an ordinary phase-matching regime, let the interfaces of each domain be parallel to the y-z plane, the optical propagation direction be along the x axis, and the directions of electric fields be along the z axis (see Fig. 2). Here, three optical fields must be taken into account, one for $\omega_1=\omega$, one for $\omega_2=2\omega$, and one for $\omega_3=3\omega$. The three optical fields, described in terms of their electric field components, are given by

$$E_i(x,t)=E_i(x)\exp[i(\omega_i t-k_i x)], \quad i=1,2,3 \tag{3}$$

which satisfy the wave equation

$$\nabla^2\mathbf{E}=\frac{l}{c^2}\frac{\partial^2}{\partial t^2}(\varepsilon\mathbf{E}+4\pi\mathbf{p}_{\mathrm{NL}}) \ . \tag{4}$$

The presence of these electric fields can give rise to nonlinear polarizations at frequencies w_2 and w_3, etc., which are

$$\begin{aligned} P_{2\omega}(x,t)&=2d(x)E_1^2(x)\exp[i(2\omega_1 t-2k_1 x)] \ , \\ P_{3\omega}(x,t)&=4d(x)E_1(x)E_2(x) \\ &\quad\times\exp\{i[(\omega_1+\omega_2)t-(k_1+k_2)x]\} \ , \end{aligned} \tag{5}$$

where

$$d(x)=\begin{cases} d_{33} & \text{if } x \text{ is in the positive domains} \\ -d_{33} & \text{if } x \text{ is in the negative domains} \ . \end{cases}$$

Before going into a detailed analysis, we must make some assumptions. We assume that the variation of the field amplitudes with x is small enough so that $k_i\,dE_i/dx \gg d^2E_i/dx^2$ and that the amount of power lost from the input beam (ω_1) is negligible, i.e., $dE_1(x)/dx=0$. We also assume that $E_1 \gg E_2$, E_3; this is the so-called small-signal approximation.

Under these conditions, using Eqs. (3)–(5) and carrying out the indicated differentiation, we can get[11]

$$dE_1(x)/dx=0 \ , \tag{6a}$$

$$\begin{aligned} dE_2(x)/dx&=-i\frac{8\pi\omega_2^2}{k^{2\omega}c^2}d(x)E_1^2(x) \\ &\quad\times\exp[i(k^{(2\omega)}-2k^{(\omega)})x] \ , \end{aligned} \tag{6b}$$

$$\begin{aligned} dE_3(x)/dx&=-i\frac{16\pi\omega_3^2}{k^{3\omega}c^2}d(x)E_1(x)E_2(x) \\ &\quad\times\exp[i(k^{(3\omega)}-k^{(2\omega)}-k^{(\omega)})x] \ . \end{aligned} \tag{6c}$$

In Eqs. (6), only the largest terms have been kept.

By integrating Eqs. (6), the electric fields after passing

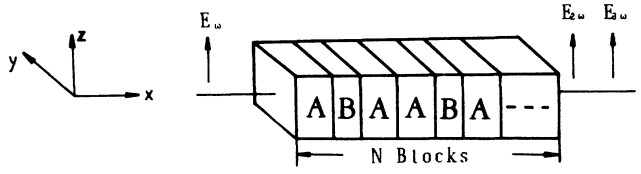

FIG. 2. The polarization orientation of electric fields with respect to the superlattice.

through the OFS can be represented as

$$E_1(x_N)=E_1 , \tag{7a}$$

$$E_2(x_N)=\sum_{i=1}^{N} E_2^i \exp(i\,\Delta k\, x_{i-1}) , \tag{7b}$$

$$E_3(x_N)=-i\frac{144\pi\omega^2}{k^{3\omega}c^2}E_1\int_0^{x_N} d(x)E_2(x') \times\exp(i\,\Delta k' x')dx' , \tag{7c}$$

where

$$\Delta k = k^{(2\omega)}-2k^{(\omega)} ,$$

$$\Delta k' = k^{(3\omega)}-k^{(2\omega)}-k^{(\omega)} ,$$

$$0.25K_1=(32\pi\omega^2 d_{33}/k^{(2\omega)}c^2\Delta k)E_1^2 ,$$

$$E_2^i=0.25K_1[1-2\exp(i\,\Delta k\, l)+\exp(i\,\Delta k\, L)] .$$

When $L=l_A=l_A^+ +l_A^-$, $E_2^i=E_2^A$, which suits block A, and when $L=l_B=l_B^+ +l_B^-$, $E_2^i=E_2^B$, which suits block B. In deriving Eq. (7), the boundary conditions have been used, which are $E_1(0)=E_1$, $E_2(0)=0$, $E_3(0)=0$.

These equations constitute the basis of our numerical calculations and discussions of this paper. We will discuss them in detail in the following section.

III. NUMERICAL CALCULATIONS AND DISCUSSIONS

We have performed numerical computations for both SHG and THG with the pump beam at a wavelength 1.318 μm of a neodymium-doped yttrium aluminum garnet (Nd:YAG) laser. For $LiNbO_3$ crystals, under room temperature, the refractive indices, according to Hobden and Warner's equation,[12] are

$n_o=2.2215$, $n_e=2.1436$ at $\lambda=1.318$ μm ,

$n_o=2.2839$, $n_e=2.1953$ at $\lambda=0.659$ μm ,

$n_o=2.3913$, $n_e=2.2882$ at $\lambda=0.439$ μm .

A. Second-harmonic generation

SHG is the result of two intense pump beams mixing. Under the condition of the small-signal approximation, the second-harmonic intensity depends completely on the structures of the superlattice.

Figure 3 shows the relationship between the second-harmonic intensity and the block nubmer with $l=l_c^{(2\omega)}=\pi/\Delta k$, $t=\tau$, and δ taking various values. Note that when $\delta=0$, the enhancement of the second-harmonic intensity is proportional to the square of the block number as curve a of Fig. 3 indicates. It is just the result of a periodic one. For when $\delta=0$, the OFS turns back to a periodic optical superlattice (POS) (see Eq. (1)]. Curves b and c represent the enhancement of the second-hamonic intensity with $\delta=0.15$ and 0.30. The curve of $\delta=0.15$ grows more slowly than the square dependence curve a, but more rapidly than the curve of $\delta=0.30$.

If the thicknesses of the domains do not have regularities like those of OFS and POS, but are radomly distributed around the coherent length as illustrated in Fig. 1(d), i.e., an aperiodic optical superlattice (APOS), the second-harmonic intensity will be linearly dependent on the number of blocks[7] (see Fig. 3, curve d).

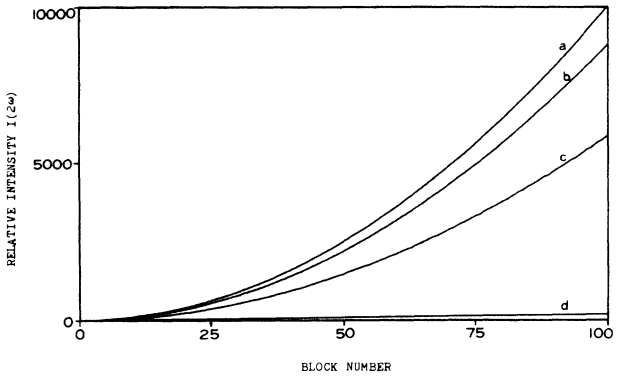

FIG. 3. The dependence of the second-harmonic intensity on the block number with $l=6.37$ μm in different cases. a, $\delta=0$, i.e., in a POS; b, $\delta=0.15$, i.e., in an OFS; c, $\delta=0.30$, i.e., in an OFS; d, in an APOS.

Compared with those of POS and APOS, the enhancement of the second-harmonic intensity of the OFS with an arbitrary value of δ can be represented as

$$I_{2\omega}(N)\propto N^{\alpha} , \tag{8}$$

with $1<\alpha<2$.

We know that the symmetry of the POS is the highest of the three, and the next highest is the OFS. The symmetry of the APOS is the lowest. From our discussion, the enhancement of the second-harmonic intensity is clearly related to the symmetry of the superlattice in which the parametric process takes place.

B. Third-harmonic generation

The process of THG discussed here is a coupled parametric process; that is, two parametric processes, the SHG process and the frequency up-conversion process (FUP), which mixes the fundamental frequency with the second harmonic, are coupled in this material.

Taking $l=l_c^{(2\omega)}=\pi/\Delta k$ and $l=5.98$ μm, we have calculated the dependence of the third-harmonic intensity on the block number, which is shown in Fig. 4. The two curves differ from each other in nature completely; one fluctuates drastically while the other increases steadily with the block number. The explanation is as follows.

As discussed above, when $l=l_c^{(2\omega)}=6.37$ μm and $\delta=0$, the second harmonic is quasi-phase-matched. However, when δ is small and $l=l_c^{(2\omega)}$, the second-harmonic intensity still increases with the block number and reaches a degree to be used practically, as Fig. 3 shows. But then the third harmonic is not quasi-phase-matched. In some parts of the superlattice, the third harmonic is constructive, and in other parts of the superlattice it is destructive. So its intensity fluctuates drastically as the block number varies. Curve a of Fig. 4 shows this feature clearly. But from Eq. (7) we can see that the THG depends

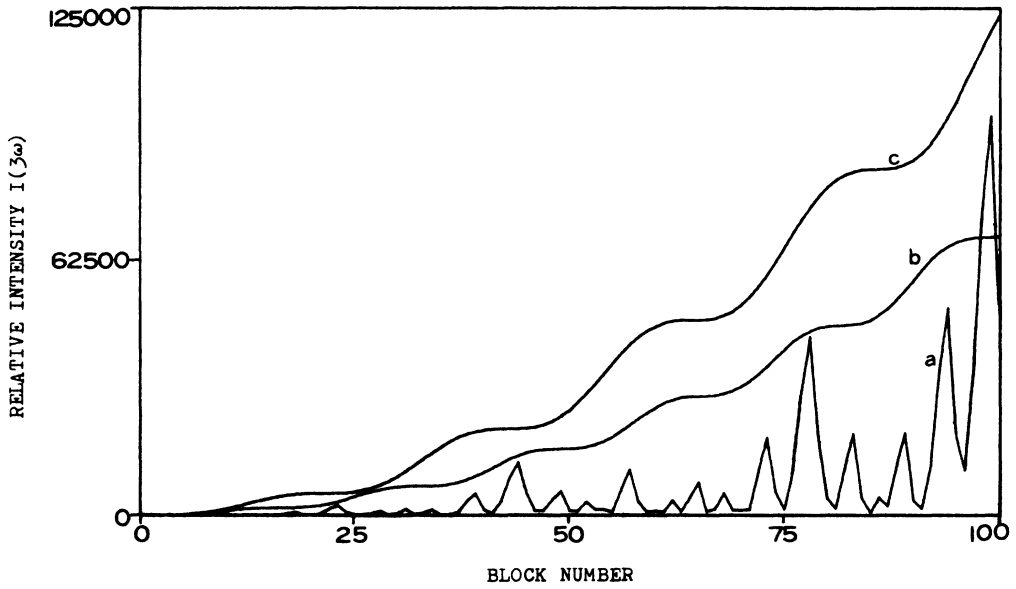

FIG. 4. The dependence of the third-harmonic intensity on the block number under different conditions. *a*, $l=6.37$ μm, $\delta=-0.10$, $t=1.62$; *b*, $l=5.98$ μm, $\delta=-0.02$, $t=1.78$; *c*, $l=6.08$ μm, $\delta=0.01$, $t=1.90$.

not only on the structure parameters but also on the second-harmonic intensity. So as the block number increases, the third-harmonic intensity undulates more severely while the second-harmonic intensity increases steadily.

When $l=5.98$ μm, we find that

$$\Delta k' l = 3\pi \ . \tag{9}$$

Therefore, $l=3l_c^{(3\omega)}$; here $l_c^{(3\omega)}$ represents the coherent length for the THG in a single FUP. The reason why l should assume a value three times $l_c^{(3\omega)}$ is obvious. Because, if $l=l_c^{(3\omega)}$, the THG in a single FUP is quasi-phase-matched, but the SHG is severely phase mismatched. The result is that it is impossible to get efficient THG because of its relation to the SHG. We know the effect of $l=3l_c^{(3\omega)}$ is the same as the effect of $l=l_c^{(3\omega)}$ for THG. And when $l=3l_c^{(3\omega)}$, the mismatch of the SHG becomes smaller. Thus the third-harmonic intensity increases with the block number (Fig. 4 curve *b*).

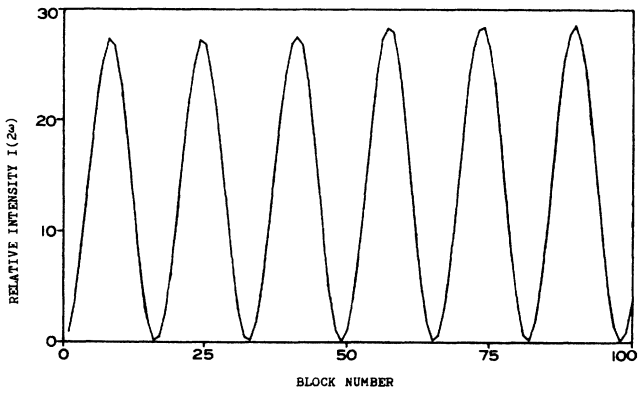

FIG. 5. The dependence of the second-harmonic intensity on the block number with $l=5.98$ μm, $\delta=-0.02$, and $t=1.78$.

Curve *b* of Fig. 4 has a steplike shape. In this case, the second harmonic is phase mismatched. Figure 5 reveals this feature. The second-harmonic intensity fluctuates almost sinusoidally. There is a one-to-one correspondence between Fig. 5 and curve *b* of Fig. 4. Whenever the second-harmonic intensity decreases, a platform appears on the third-harmonic intensity. This strongly indicates the dependence of THG on SHG.

By adjusting the parameters properly, the optimum condition has been found, which is $l=6.08$ μm, $\delta=0.01$, and $t=1.90$ with the third-harmonic intensity $I_{3\omega}\approx 122\,000K_2^2$; here $K_2=576\pi\omega^2 d_{33}K_1E_1/(k^{(3\omega)}c^2\Delta k')$ (Fig. 4, curve *c*).

To obtain an appreciation for the enhancement of the third harmonic available in our case, consider a commonly used two-step process.[13] The second harmonic is generated in the first $LiNbO_3$ crystal of $100l_c^{(2\omega)}$ length using the nonlinear coefficient d_{31} with phase matching; then it mixes with the fundamental frequency in the second $LiNbO_3$ crystal of $100l_c^{(3\omega)}$ length using the same nonlinear coefficient; here $l_c^{(3\omega)}=\pi/\Delta k'$, and the relative output intensity of THG is $I_{3\omega}\approx 11\,000K_2^2$. Compared with it, the enhancement of THG in our case is increased by an order of magnitude, which is favorable to the practical applications.

IV. CONCLUSION

We have presented a detailed theoretical analysis of SHG and THG in the OFS, and particularly considered an OFS made from a single $LiNbO_3$ crystal with quasi-periodic laminar ferroelectric-domain structures as an example.

The analysis used here can be carried over to the OFS of other materials. The deal with OFS's which consist of different materials with different refractive indices along the optical propagation direction, the reflection by the interfaces must be considered.

The OFS discussed here is a new solution to the phase mismatch of the optical parametric processes. With this material, not only might SHG and THG have applicable enhancement, but also other parametric processes might proceed with large enhancement.

ACKNOWLEDGMENTS

This work was supported by the Chinese National Natural Science Foundation.

---

*To whom all communications regarding this paper should be addressed.

[1]J. A. Armstrong, N. Bloembergen, J. Ducuing, and P. S. Pershan, Phys. Rev. **127**, 1918 (1962).

[2]N. Bloembergen and A. J. Sievers, Appl. Phys. Lett. **17**, 483 (1970).

[3]D. Feng, N. B. Ming, J. F. Hong, Y. S. Yang, J. S. Zhu, Z. Yang, and Y. N. Wang, Appl. Phys. Lett. **37**, 607 (1980).

[4]Y. H. Xue, N. B. Ming, J. S. Zhu, and D. Feng, Wuli Xuebao (Acta Phys. Sin.) **32**, 1515 (1983) [Chin. Phys. **4**, 554 (1984)].

[5]D. E. Thompson, J. D. McMullen, and D. B. Anderson, Appl. Phys. Lett. **29**, 113 (1973).

[6]M. Okada, K. Takizawa, and S. Ieiri, NKH (Nippon Hoso Kyokai) Tech. J. **29**, 24 (1977).

[7]C. F. Dewey and L. O. Hocker, Appl. Phys. Lett. **26**, 442 (1975).

[8]D. Levine and P. J. Steinhardt, Phys. Rev. Lett. **53**, 2477 (1984).

[9]R. K. Zia and W. J. Dallas, J. Phys. A **18**, L341 (1985).

[10]Veit. Elser, Phys. Rev. B **32**, 4892 (1985).

[11]F. Zernike and J. M. Midwinter, *Applied Nonlinear Optics* (Wiley, New York, 1973).

[12]M. V. Hobden and J. Warner, Phys. Lett. **22**, 243 (1966).

[13]R. Piston, Laser Focus **14**, 66 (1978).